2012 IEEE/RSJ International Conference on
Intelligent Robots and Systems
October 7-12, 2012. Vilamoura, Algarve, Portugal

Dynamic Model of Three Wheeled Narrow Tilting Vehicle and Corresponding Experiment Verification

Hiroki Furuichi, Jian Huang, *Member, IEEE*,
Takayuki Matsuno, *Member, IEEE* and Toshio Fukuda, *Fellow, IEEE*

***Abstract*— The traffic congestion is growing in urban area these days due to the rapidly increasing number of automobiles. One of the traffic problem solutions is to increase the flow rate of a particular traffic artery. To make the vehicle smaller and narrower might be a good idea. We developed a new conceptual Narrow Tilting Vehicle (NTV) that has one front wheel and two rear wheels. The proposed NTV is very narrow and all three wheels can tilt to improve the stability during turning. We also derive a new switching dynamical model of the NTV. This model considers several states including normal running, temporary running with one rear wheel not on the ground and totally falling down. Based on this model, a simulation platform is established, which is useful to test different control methods and to investigate dangerous driving situations in case hurt drivers in real experiments. The effectiveness of proposed dynamical model is verified through comparison study of simulations and corresponding experiments.**

I. INTRODUCTION

An efficient approach to solve the traffic congestion is to make the vehicle smaller and narrower [1]. To build up a traffic system using narrow vehicle, a key problem we have to solve is how to develop a safe, stable and easily maneuverable narrow vehicle.

Narrow vehicles have been extensively studied in the last decade. Huang *et al.*[2] proposed a Sliding-Mode Control (SMC) approach for Mobile Wheeled Inverted Pendulum (MWIP) based on a novel sliding surface. MWIP is a model of two-wheeled vehicle which is used in the JOE[3], the Segway[4], the B2[5] etc. R. S. Sharp *et al.* built a model of two-wheeled motorcycle, based on which stable motion control method can be designed. This model is also frequently used in calculation of steady turning, stability and forces acted on the ground [6]-[9]. R. Rajamani *et al.* presented new conceptual Three-Wheeled-Vehicle (TWV) called Narrow Commuter Vehicle (NCV). This NCV can tilt all three wheels so that it can turn around in a fast speed at the corner. Their NCV has two front wheels and one rear wheel[10]-[12]. There are several kinds of TWV whose shape is narrow and all three wheels can tilt. Generally we call these TWV as Narrow-Tilt-Vehicle (NTV). In this paper, we focus on the NTV which has one front wheel and two rear wheels.

Stability problem is one of the most important problems in delivering a traffic system using NTVs. To guarantee the stability, our goal is to control the NTV not to turn down even if one of the rear wheels is not on the ground. This situation often happens when the NTV turns around suddenly at a high speed. Although there are a lot of models for single track vehicles, to our knowledge few of them can be used to describe the NTV with one wheel not contacting ground. Thus, this paper aims to propose a new switching dynamical model considering several NTV running states including normal running, temporary running with one rear wheel not on the ground and totally falling down. Based on this model, a simulation platform is establish to simulate control of NTV. This simulation is significant for investigating dangerous driving situations in case hurt drivers in real experiments. Section II gives the mechanical structure of our NTV. In Section III, the model formulations of our new switching dynamical model of NTV is discussed. By using this new dynamical model, we made a simulation platform in MATLAB which can be used to analyze typical dynamical behaviors of NTV. Finally, we verify the effectiveness of proposed model and simulation platform through comparison study of simulations and corresponding experiments.

II. MECHANICAL STRUCTURE OF NTV

In this study, we focus on the NTV which has one front wheel and two rear wheels. Advantages of such structures is that maneuverability of vehicle is good and it can be operated in the same way as bicycles or motorbikes so that the vehicle will be zippy. The two rear wheels may be actively tilted by a motor fixed on the rear part. The steering angle and moving velocity of NTV can also be measure as inputs to control the tilt angle. Fig. 1 shows the tilting concept of the NTV. All wheels will tilt when it turns around. This increases the stability when it turns around and makes it possible to curve at a high speed. Fig. 2 and 3 show the schematic view and picture of our NTV. Some notations describing the NTV parameters should be clarified first, which are listed as follows:

1) b - width of the vehicle;
2) h - height of the COG (Center Of Gravity) of the vehicle;
3) r_{fw} - radius of the front wheel;

Manuscript received 10 March, 2012. This work was supported by Equos Research Co., Ltd.

H. Furuichi and T. Fukuda are with the Department of Micro-Nano Systems Engineering, Nagoya University, Furo-cho-1, Chikusa-ku, Nagoya, Aichi, 464-8603, JAPAN (phone: +81-52-789-4481; fax: +81-52-789-3115) furuichi@robo.mein.nagoya-u.ac.jp, fukuda@mein.nagoya-u.ac.jp

J. Huang is with the Department of Control Science and Engineering, Huazhong University of Science and Technology, Wuhan 430074, CHINA huang_jan@mail.hust.edu.cn

T. Matsuno is with the Department of Natural Science and Technology, Okayama University, Tsushimanaka3-1-1, Kita-ku, Okayama, Okayama, 700-8530, JAPAN matsuno@cc.okayama-u.ac.jp

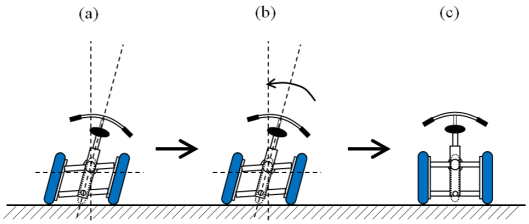

Fig. 1. Tilting concept of Narrow Tilting Vehicle. (rear view of the vehicle)

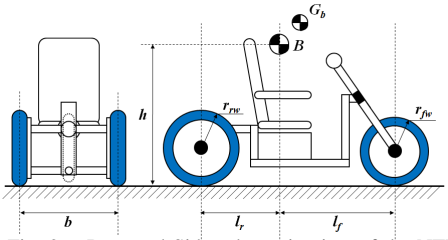

Fig. 2. Rear and Side schematic view of the NTV

Fig. 3. Picture of the NTV

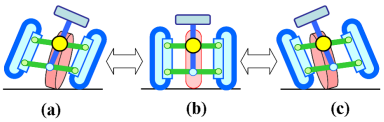

Fig. 4. Three tolerant running states of NTV (rear view)

4) r_{rw} - radius of the rear wheel;
5) l_f - length from center of the front wheel to COG;
6) l_r - length from center of the rear wheel to COG;
7) B - point of COG of total vehicle;
8) G_b - point of COG of body part.

More details about notations are illustrated in the Appendix.

III. Model Formulation of NTV

We can categorize the running states of our NTV into the following types:

T1) Temporary running with left rear wheel not on the ground (Fig . 4-a).

T2) Normal running with all wheels on the ground (Fig. 4-b).

T3) Temporary running with right rear wheel not on the ground (Fig. 4-c).

T4) Totally fall down.

In existing modeling work of three-wheeled NTV, e.g. in [12], researchers only paid attention to normal state T2. Whereas, State T1 and T3 often occur when the NTV turns around suddenly at a high speed. These states are intermediate states between T2 and T4, and are important in the stability analysis. Thus, in this study we aim at establishing a switching system model for NTV, which can describe these three tolerable running states.

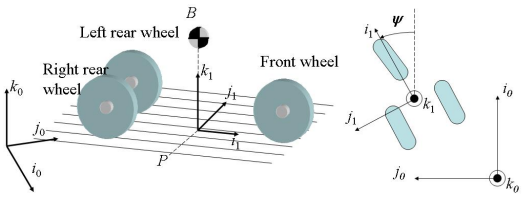

(a) Full view (b) Top view

Fig. 5. Coordinates systems $\{0\}$ and $\{1\}$

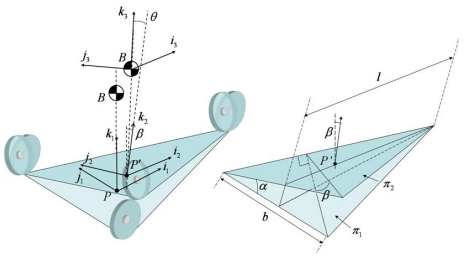

Fig. 6. Coordinates systems $\{1\}$, $\{2\}$ and $\{3\}$. Full view of NTV with right wheel lifted

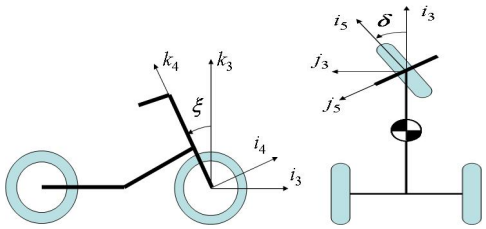

(a) Side view (b) Top view

Fig. 7. Coordinates systems $\{3\}$, $\{4\}$ and $\{5\}$

A. Coordinate Definition

Note that dynamical model of T1 can be obtained in the similar way to computing model of T3, and dynamical model of T2 is a special case of state T3. To simplify the illustration, we only give the modeling procedure of state T3 in this paper. All coordinate definitions are given as follows.

We consider system $\{0\}$ to be the inertial frame while system $\{1\}$ is non-inertial in that it has an instantaneous rotation of $\dot{\psi}$ around k_0 and instantaneous translation of $\dot{y}$ in j_0 direction.

In the case of the NTV lifts up its right wheel from the ground, the supporting surface π_1 will rotate angle β around the axis crossing two contact points between the ground and the other two wheels. We denote the new surface by π_2 and define a new system $\{2\}$ fixed to π_2 corresponding system $\{1\}$ fixed on π_1. The next useful coordinate system is system $\{3\}$. This system is fixed to the vehicle body and is formed by a rotation of θ around i_2.

Coordinate frame $\{1\}$ rotates with the yawing motion of the body while frame $\{3\}$ rotates with the rolling motion of

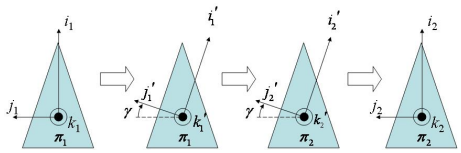

Fig. 8. Coordinates systems {1}, {1'}, {2'} and {2}

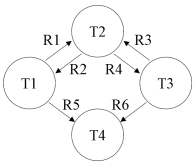

Fig. 9. State transition diagram of NTV

the body. The front wheel has one degree of freedom with respect to the vehicle body. We define two more coordinate frames to deal with this. The first is the steering axis of the front wheel which is oriented at an angle ξ from the k_3 (Fig. 7-a). The last system $\{5\}$ is defined from the steering angle δ (Fig. 7-b).

To calculate the rotation matrix from $\{1\}$ to $\{2\}$, we also define two more systems $\{1'\}$ and $\{2'\}$, which are depicted in Fig. 8. All rotation matrices can be easily obtained.

B. Dynamical Model of State T3

Some assumptions to avoid the complexity of the model are assumed in this paper, which are listed as follows.

1) The steer axis is perpendicular to the ground, i.e., system $\{4\}$ is coincident with system $\{3\}$.
2) The weights of wheels are much less than the body. We use nonholonomic constraints and the equations would be too complex without this.
3) The vehicle is moving at a constant speed. This is because the actual vehicle has varying velocity and needed to be closed loop to get a long enough sample.
4) The external forces on two rear wheels are same in state T2. This is because we cannot measure the accurate force from the ground.

Also, we assume that there are no influence of driver. It means there are no influence of the travel of COG by the driver. To derive the dynamic model of NTV, general equations of motion using Newton-Euler Method are,

$$m\mathbf{a}^G = \mathbf{F} \tag{1}$$

$$\frac{d}{dt}\mathbf{H}^G = \mathbf{M} \tag{2}$$

where m is the mass, $\mathbf{a}^G$ is the acceleration of COG, $\mathbf{F}$ is the resultant force, $\mathbf{H}^G$ is the angular momentum at COG, $\mathbf{M}$ is the resultant moments.

Each term of these equations is a vector in 3D space. Also, note that all of the symbols in the equations are given in the Appendix.

To derive the dynamical model, we used Transport Theorem[13]. Similar to the modeling procedure in [12], we can calculate the acceleration $\mathbf{a}^G$, the angular momentum $\mathbf{H}^G$, the external resultant force $\mathbf{F}$, the external resultant moment $\mathbf{M}$ for each parts of the NTV. After combining the equations of all parts, the motion equations of lateral translation y, roll motion β, yaw motion ψ can be obtained as follows:

$$\begin{aligned} C_\gamma \cdot \ddot{y} = {} & (\bullet)_1 \cdot S_\gamma C_\beta + (\bullet)_2 \cdot C_\gamma C_\beta + (\bullet)_3 \cdot S_\beta \\ & - \ddot{\beta}(n_{\beta 1} \cdot S_\gamma C_\beta + n_{\beta 2} \cdot C_\gamma C_\beta + n_{\beta 3} \cdot S_\beta) \\ & - \ddot{\psi}(n_{\psi 1} \cdot S_\gamma C_\beta + n_{\psi 2} \cdot C_\gamma C_\beta + n_{\psi 3} \cdot S_\beta) \\ & - \ddot{\theta}(n_{\theta 1} \cdot S_\gamma C_\beta + n_{\theta 2} \cdot C_\gamma C_\beta + n_{\theta 3} \cdot S_\beta) \end{aligned} \tag{3}$$

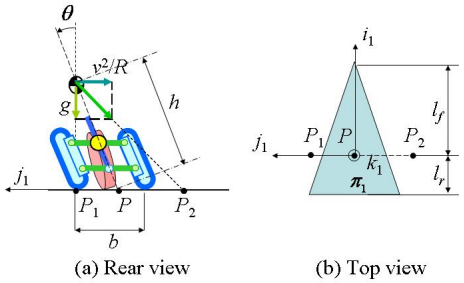

(a) Rear view (b) Top view

Fig. 10. Lateral acceleration analysis when NTV turns around. P_1 is the projection of NTV COG to the ground. P_2 is the projection of resultant lateral acceleration of NTV COG. R is the turning radius. g denotes the gravity.

$$\begin{aligned} & \{-n_{\beta 1} \cdot mhS_\gamma C_\theta - n_{\beta 2} \cdot mhC_\gamma C_\theta \\ & \qquad - n_{\beta 3} \cdot m(l_f S_\gamma - hC_\gamma S_\theta) + e_{\beta 1}\}\ddot{\beta} \\ & = -(\bullet)_1 \cdot mhS_\gamma C_\theta - (\bullet)_2 \cdot mhC_\gamma C_\theta \\ & \qquad - (\bullet)_3 \cdot m(l_f S_\gamma - hC_\gamma S_\theta) + (\bullet)_4 \\ & - \ddot{y}\{-n_{y1} \cdot mhS_\gamma C_\theta - n_{y2} \cdot mhC_\gamma C_\theta \\ & \qquad - n_{y3} \cdot m(l_f S_\gamma - hC_\gamma S_\theta)\} \\ & - \ddot{\psi}\{-n_{\psi 1} \cdot mhS_\gamma C_\theta - n_{\psi 2} \cdot mhC_\gamma C_\theta \\ & \qquad - n_{\psi 3} \cdot m(l_f S_\gamma - hC_\gamma S_\theta) + e_{\psi 1}\} \\ & - \ddot{\theta}\{-n_{\theta 1} \cdot mhS_\gamma C_\theta - n_{\theta 2} \cdot mhC_\gamma C_\theta \\ & \qquad - n_{\theta 3} \cdot m(l_f S_\gamma - hC_\gamma S_\theta) + e_{\theta 1}\} \end{aligned} \tag{4}$$

$$\begin{aligned} (e_{\psi 2} \cdot S_\beta - e_{\psi 3} \cdot C_\beta) \cdot \ddot{\psi} = {} & (\bullet)_5 \cdot S_\beta - (\bullet)_6 \cdot C_\beta \\ & - \ddot{\beta}(e_{\beta 2} \cdot S_\beta - e_{\beta 3} \cdot C_\beta) \\ & - \ddot{\theta}(e_{\theta 2} \cdot S_\beta - e_{\theta 3} \cdot C_\beta) \end{aligned} \tag{5}$$

All items in (3-5) are given in the Appendix. The motion equation of tilt angle θ is not calculated because we use an active tilt controller and the dynamics of θ can be approximated by a linear motor model.

C. Switching Conditions for Models of Different States

The state transition diagram of NTV is shown in Fig. 9. To obtain the state switching conditions, the lateral acceleration of NTV is analyzed when it turns around. As shown in Fig. 10, the total lateral acceleration includes two parts: the gravity g and the centrifugal acceleration. The latter can be calculated by v^2/R. Obviously, a state transition from T2 to T1 will occur if P_2 goes right and outside the support triangle. Similarly, all the switching conditions can be easily obtained.

D. Total Control Diagram

As shown in Fig. 10, the NTV system will be in state T2 which is in stable motion if point P_2 always locates inside the support triangle π_1. As Yi did in [14], we can approximately compute P_2 as

$$P_2 = hsin\theta - \frac{v^2 htan\delta}{gl} \tag{6}$$

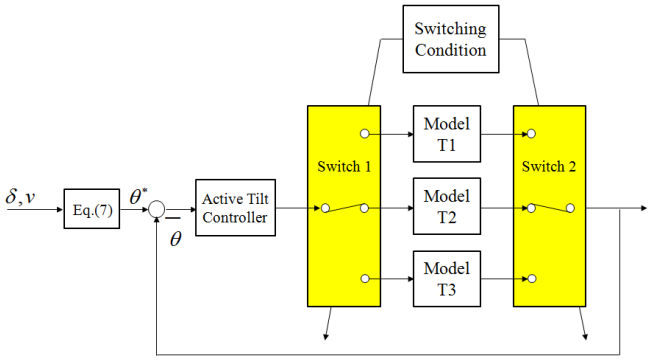

Fig. 11. Control diagram of NTV

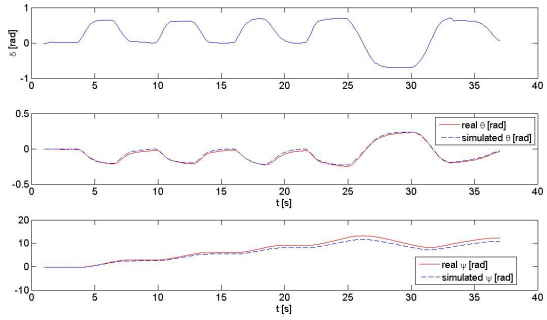

Fig. 12. Comparison of experimental and simulated trajectories of NTV when it runs in state T2

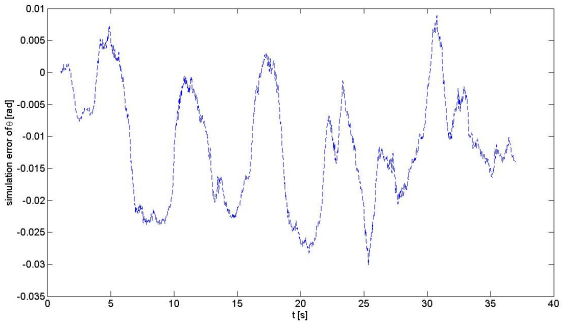

Fig. 13. Simulation error of tilt angle θ of NTV when it runs in state T2

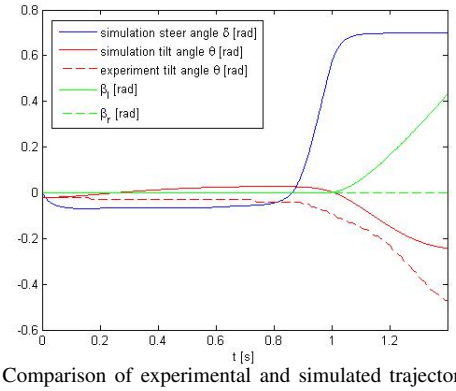

Fig. 14. Comparison of experimental and simulated trajectories of NTV in a T2 → T1 switching case

To stabilize the system, the desired position of P_2 is the original point O. Therefore, the desired tilt angle θ^* is given by

$$\theta^* = sin^{-1}(\frac{v^2 tan\delta}{gl}) \tag{7}$$

This desired tilt angle is a function of current steering angle δ and the moving velocity v of NTV. The total control diagram of NTV is illustrated by Fig. 11.

IV. Simulation and Experiment Study

To verify the correctness of our proposed switching model, some simulations and corresponding experiments are performed on the NTV. In all the simulations, the control diagram shown by Fig. 11 is implemented in MATLAB/SIMULINK. The active tilt controller is chosen as a conventional PI control. The tilt dynamics of θ is approximated by a second-order transfer function tilt motor model, which is identified offline.

A. Simulation and Experiment of Model T2

In most of the driving time, the NTV runs in state T2. That is, all wheels are on the ground. We first verify our switching model in this special case. Both experiment and simulation were performed. In the experiment, a driver was asked to ride the NTV at will in an almost constant velocity. All real-time NTV parameters were recorded simultaneously. In the simulation, the real steering angle δ and driving velocity v were input to our switching model in SIMULINK. Corresponding motion state variables were obtained. The real steering angle trajectory and comparison results of simulation and experiment are shown in Fig. 12. It turns out that the simulated tilt angle trajectory matches the real one well. The maximum simulation error of θ is less than 0.01 rad (see Fig. 13). For the yaw angle ψ, the simulation error will accumulate along the driving time. However, this accumulated error does not affect the system stability. Therefore, we can say that our proposed model and the simulation platform are effective at least in the normal driving state.

B. Simulation and Experiment of Two State Switching

To further verify our dynamics and the switching model, we also investigated the 2-state switching situation. In the experiment, the NTV runs straightly at a constant speed (20 km/h), then turns on a dime to the left. The recorded real steering angle δ and velocity v were input to the model in SIMULINK.

The comparison results of simulation and experiment are shown in Fig. 14. From the simulated trajectory of roll angle β_r, the NTV starts raising its left rear wheel approximately at instant $t = 1$ [sec]. This is very coincident with what we have observed from the experiment. The trend of experimental and simulated tilt angle θ matches each other too while simulation error exists. These errors do not affect the stability analysis since the dynamic responses are almost same in the simulation and experiment. At the end of this experiment, the NTV fell down to the right, which is exactly same as the result of simulation (see Fig. 15). These facts demonstrate that our proposed switching model is effective to reflect physical state transition and dynamic response of a NTV.

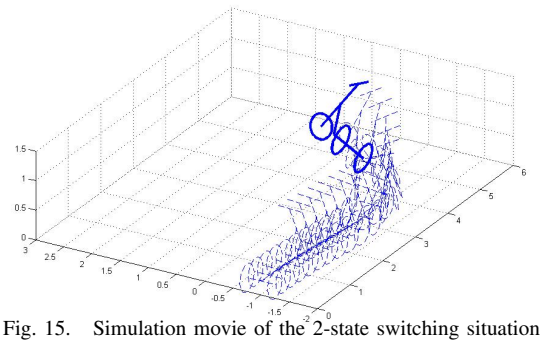

Fig. 15. Simulation movie of the 2-state switching situation

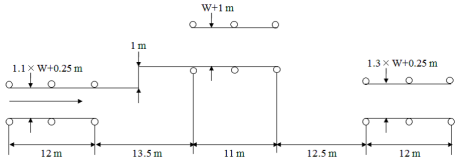

Fig. 16. ELK test course

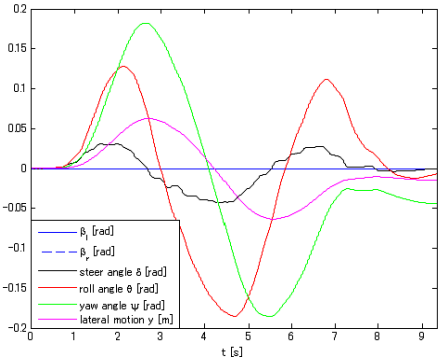

Fig. 17. Simulation data of ELK test at 30[km/h]

C. ELK Test Simulation of NTV

ELK test is a test to determine how a certain vehicle acts when the driver evades a suddenly appearing obstacle and it is widely used to test the stability of the vehicle [15]. To perform an ELK test at a high speed is dangerous for the driver. Therefore, we applied our simulation platform to analyze the NTV stability at different velocities. Two constant velocities, 30 km/h and 60 km/h, are evaluated in the simulation. Fig. 16 shows the schematic of the ELK test course. Fig. 17 shows the simulation data of ELK test at v=30[km/h]. As we can see, both roll angles β_l and β_r are always zero, which means that all wheels of NTV are on the ground all the time during the test. This result is coincident with the experience of NTV driver. Fig. 18 shows the simulation data of ELK test at v=60[km/h]. We found that state transitions occur around instant t = 1.3 s (T2 $\rightarrow$ T3) t = 1.8 s (T3 $\rightarrow$ T2) and t = 2.4 s (T2 $\rightarrow$ T1). The NTV finally fall down because roll angle β_l increases fast after the last transition. This means the ELK test fails at a high velocity and matches the driver's experience too. In these simulation, all state transitions occurred. This also implies the effectiveness our switching NTV model for describing

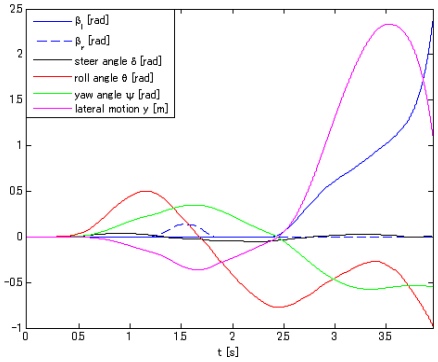

Fig. 18. Simulation data of ELK test at 60[km/h]

physical state switching.

V. CONCLUSIONS

In this paper, we proposed a switching dynamical model for Narrow-Tilting-Vehicles (NTV). Several running states of NTV, including normal running, temporary running with left rear wheel not on ground, temporary running with right rear wheel not on ground and totally falling down, are involved in the model. By using this model, a simulation platform is established in MATLAB/SIMULINK. Comparison studies of several simulations and corresponding experiments are performed to demonstrate the effectiveness of our proposed model. Simulation of ELK test of NTV is also done and the results are coincident with the driver's experiences. The proposed model and simulation platform are significant to test different control methods and to investigate dangerous driving situations in case hurt drivers in real experiments. Comparing the ELK test simulation result and the experiment data of running the ELK test course is one of our future work.

VI. APPENDIX

A. Notation

- $\frac{d}{dt}^n x$: Time derivative of vector x with respect to frame n
- ${}^J\mathbf{r}^I$: Position of point I with respect to J respectively
- b, rlw, rrw, fw : Subscripts indicating vehicle body, rear left or right wheels, and front wheel respectively

B. Vehicle Specific Symbols

1) Constant Terms:

- $G_b, G_{rlw}, G_{rrw}, G_{fw}$: Point of of center of gravity of individual bodies
- m : Mass of the vehicle
- $I_b^{xx}, I_b^{yy}, I_b^{zz}$: Moments of inertia of vehicle body about each directions
- S_γ, C_γ : Abbreviation of $sin(\gamma)$ and $cos(\gamma)$

2) State Dependent Terms:

- n_{y1}, n_{y2}, n_{y3} :
  $n_{y1} = S_\gamma C_\gamma (C_\beta - 1)$, $n_{y2} = S_\gamma^2 + C_\gamma^2 C_\beta$, $n_{y3} = C_\gamma S_\beta$
- $n_{\theta 1}, n_{\theta 2}, n_{\theta 3}$:
  $n_{\theta 1} = 0$, $n_{\theta 2} = hC_\theta$, $n_{\theta 3} = -hS_\theta$
- $n_{\psi 1}, n_{\psi 2}, n_{\psi 3}$:
  $n_{\psi 1} = l_r S_\gamma C_\gamma (1 - C_\beta) - \frac{b}{2} C_\gamma^2 (1 - C_\beta) + h(-C_\gamma S_\beta C_\theta - C_\beta S_\theta)$
  $n_{\psi 2} = -l_r S_\gamma^2 (1 - C_\beta) + \frac{b}{2} S_\gamma C_\gamma (1 - C_\beta) + hS_\gamma S_\beta C_\theta$
  $n_{\psi 3} = -hS_\gamma S_\beta S_\theta$

- $n_{\beta 1}, n_{\beta 2}, n_{\beta 3}$:
  $n_{\beta 1} = hS_\gamma C_\theta, n_{\beta 2} = hC_\gamma C_\theta$, $n_{\beta 3} = -hC_\gamma S_\theta - l_r S_\gamma + \frac{b}{s} C_\gamma$
- $e_{\psi 1}, e_{\psi 2}, e_{\psi 3}$:
  $e_{\psi 1} = -I_b^{xx} S_\gamma C_\gamma S_\beta + I_b^{yy}(S_\gamma C_\gamma S_\beta C_\theta^2 + S_\gamma C_\beta S_\theta C_\theta) + I_b^{zz}(S_\gamma C_\gamma S_\beta S_\theta^2 - S_\gamma C_\beta S_\theta C_\theta)$
  $e_{\psi 2} = -I_b^{xx} S_\gamma^2 S_\beta + I_b^{yy}(-C_\gamma^2 S_\beta C_\theta^2 - C_\gamma C_\beta S_\theta C_\theta) + I_b^{zz}(-C_\gamma^2 S_\beta S_\theta^2 + C_\gamma C_\beta S_\theta C_\theta)$ $e_{\psi 3} = I_b^{yy}(C_\gamma S_\beta S_\theta C_\theta + C_\beta S_\theta^2) + I_b^{zz}(-C_\gamma S_\beta S_\theta C_\theta + C_\beta C_\theta^2)$
- $e_{\theta 1}, e_{\theta 2}, e_{\theta 3}$:
  $e_{\theta 1} = -I_b^{xx} C_\gamma$, $e_{\theta 2} = -I_b^{xx} S_\gamma$, $e_{\theta 3} = 0$
- $e_{\beta 1}, e_{\beta 2}, e_{\beta 3}$:
  $e_{\beta 1} = -I_b^{xx} C_\gamma^2 - I_b^{yy} S_\gamma^2 C_\theta^2 - I_b^{zz} S_\gamma^2 S_\theta^2$
  $e_{\beta 2} = -I_b^{xx} S_\gamma C_\gamma + I_b^{yy} S_\gamma C_\gamma C_\theta^2 + I_b^{zz} S_\gamma C_\gamma S_\theta^2$
  $e_{\beta 3} = -I_b^{yy} S_\gamma S_\theta C_\theta + I_b^{zz} S_\gamma S_\theta C_\theta$
- $(\bullet)_1 \sim (\bullet)_3$:

$$
\begin{aligned}
(\bullet)_1 &= \tfrac{1}{m}(F_f + F_r) S_\gamma C_\gamma (C_\beta - 1) + g S_\gamma S_\beta \\
&-(\dot v - \dot\psi \dot y)(C_\gamma^2 + S_\gamma^2 C_\beta) - v\dot\psi S_\gamma C_\gamma (C_\beta - 1) \\
&-l_r \dot\beta^2 S_\gamma^2 C_\beta + \tfrac{b}{2}\dot\beta^2 S_\gamma C_\gamma C_\beta - l_r \dot\psi \dot\beta S_\gamma C_\gamma S_\beta + \tfrac{b}{2}\dot\psi\dot\beta C_\gamma^2 S_\beta \\
&-h\{-\dot\beta\dot\theta S_\gamma S_\theta - \dot\psi\dot\beta C_\gamma C_\beta C_\theta + \dot\psi\dot\theta C_\gamma S_\beta S_\theta - \dot\psi\dot\theta C_\beta C_\theta \\
&+\dot\psi\dot\beta S_\beta S_\theta\} - 2\breve H_1^x - \breve H_2^x - \breve H_3^x
\end{aligned}
$$

$$
\begin{aligned}
(\bullet)_2 &= \tfrac{1}{m}(F_f + F_r)(S_\gamma^2 + C_\gamma^2 C_\beta) + g C_\gamma S_\beta \\
&-(\dot v - \dot\psi \dot y) S_\gamma C_\gamma (C_\beta - 1) - v\dot\psi (S_\gamma^2 + C_\gamma^2 C_\beta) \\
&-l_r \dot\beta^2 S_\gamma C_\gamma C_\beta + \tfrac{b}{2}\dot\beta^2 C_\gamma^2 C_\beta + l_r \dot\psi\dot\beta S_\gamma^2 S_\beta - \tfrac{b}{2}\dot\psi\dot\beta S_\gamma C_\gamma S_\beta \\
&-h\dot\psi\dot\beta S_\gamma C_\beta C_\theta - 2\breve H_1^y - \breve H_2^y - \breve H_3^y
\end{aligned}
$$

$$
\begin{aligned}
(\bullet)_3 &= \tfrac{1}{m}(F_f + F_r) C_\gamma S_\beta - g C_\beta - (\dot v - \dot\psi \dot y) S_\gamma S_\beta \\
&-v\dot\psi C_\gamma S_\beta - l_r \dot\beta^2 S_\gamma S_\beta + \tfrac{b}{2}\dot\beta^2 C_\gamma S_\beta \\
&+h\dot\psi\dot\beta S_\gamma C_\beta S_\theta - 2\breve H_1^z - \breve H_2^z - \breve H_3^z
\end{aligned}
$$

- $(\bullet)_4 \sim (\bullet)_6$:

$$
\begin{aligned}
(\bullet)_4 &= (F_f l_f - F_r l_r) S_\gamma C_\gamma S_\beta + (F_f + F_r)(-hC_\gamma^2 S_\beta S_\theta + hC_\gamma C_\beta C_\theta) \\
&+\tfrac{b}{2} F_r C_\gamma^2 S_\beta - \breve E_1^x - C_\gamma \breve K_1^x + S_\gamma C_\theta \breve K_1^y + S_\gamma S_\theta \breve K_1^z
\end{aligned}
$$

$$
\begin{aligned}
(\bullet)_5 &= (F_f l_f - F_r l_r)(-C_\gamma^2 S_\beta) + (F_f + F_r)(hS_\gamma C_\theta - hS_\gamma C_\gamma S_\beta S_\theta) \\
&+\tfrac{b}{2} F_r S_\gamma C_\gamma S_\beta - \breve E_1^y - S_\gamma \breve K_1^x - C_\gamma C_\theta \breve K_1^y - C_\gamma S_\theta \breve K_1^z
\end{aligned}
$$

$$
\begin{aligned}
(\bullet)_6 &= (F_f l_f - F_r l_r)(S_\gamma^2 + C_\gamma^2 C_\beta) - (F_f + F_r) h S_\gamma C_\gamma S_\theta (1 - C_\beta) \\
&+\tfrac{b}{2} F_r S_\gamma C_\gamma (1 - C_\beta) - \breve E_1^z + S_\theta \breve K_1^y - C_\theta \breve K_1^z
\end{aligned}
$$

$$
\begin{aligned}
\breve E_1^x &= -I_b^{xx}\dot\psi\dot\beta S_\gamma C_\gamma C_\beta - S_\gamma C_\theta\{I_b^{yy}(-\dot\beta\dot\theta S_\gamma S_\theta \\
&-\dot\psi\dot\beta C_\gamma C_\beta C_\theta + \dot\psi\dot\theta C_\gamma S_\beta S_\theta - \dot\psi\dot\theta C_\beta C_\theta + \dot\psi\dot\beta S_\beta S_\theta)\} \\
&-S_\gamma S_\theta\{I_b^{zz}(\dot\beta\dot\theta S_\gamma C_\theta - \dot\psi\dot\beta C_\gamma C_\beta S_\theta - \dot\psi\dot\theta C_\gamma S_\beta C_\theta \\
&-\dot\psi\dot\theta C_\beta S_\theta - \dot\psi\dot\beta S_\beta C_\theta)\}
\end{aligned}
$$

$$
\begin{aligned}
\breve E_1^y &= -I_b^{xx}\dot\psi\dot\beta S_\gamma^2 C_\beta + C_\gamma C_\theta\{I_b^{yy}(-\dot\beta\dot\theta S_\gamma S_\theta \\
&-\dot\psi\dot\beta C_\gamma C_\beta C_\theta + \dot\psi\dot\theta C_\gamma S_\beta S_\theta - \dot\psi\dot\theta C_\beta C_\theta + \dot\psi\dot\beta S_\beta S_\theta)\} \\
&+C_\gamma S_\theta\{I_b^{zz}(\dot\beta\dot\theta S_\gamma C_\theta - \dot\psi\dot\beta C_\gamma C_\beta S_\theta - \dot\psi\dot\theta C_\gamma S_\beta C_\theta \\
&-\dot\psi\dot\theta C_\beta S_\theta - \dot\psi\dot\beta S_\beta C_\theta)\}
\end{aligned}
$$

$$
\begin{aligned}
\breve E_1^z &= -S_\theta\{I_b^{yy}(-\dot\beta\dot\theta S_\gamma S_\theta - \dot\psi\dot\beta C_\gamma C_\beta C_\theta + \\
&\dot\psi\dot\theta C_\gamma S_\beta S_\theta - \dot\psi\dot\theta C_\beta C_\theta + \dot\psi\dot\beta S_\beta S_\theta)\} + C_\theta\{I_b^{zz}(\dot\beta\dot\theta S_\gamma C_\theta \\
&-\dot\psi\dot\beta C_\gamma C_\beta S_\theta - \dot\psi\dot\theta C_\gamma S_\beta C_\theta - \dot\psi\dot\theta C_\beta S_\theta - \dot\psi\dot\beta S_\beta C_\theta)\}
\end{aligned}
$$

$$
\omega_a = {}^0\omega^3 = \begin{bmatrix} -\dot\beta C_\gamma - \dot\psi S_\gamma S_\beta - \dot\theta \\ \dot\beta S_\gamma C_\theta - \dot\psi C_\gamma S_\beta C_\theta - \dot\psi S_\theta C_\beta \\ \dot\beta S_\gamma S_\theta - \dot\psi C_\gamma S_\beta S_\theta + \dot\psi C_\theta C_\beta \end{bmatrix}_3
$$

$$
\omega_b = {}^0\omega^2 = \begin{bmatrix} -\dot\beta C_\gamma - \dot\psi S_\gamma S_\beta \\ \dot\beta S_\gamma - \dot\psi C_\gamma S_\beta \\ \dot\psi C_\beta \end{bmatrix}_2, \qquad \omega_a \times \mathbf{H}_b = \begin{bmatrix} \breve K_1^x \\ \breve K_1^y \\ \breve K_1^z \end{bmatrix}_3
$$

$$
\omega_b \times (\frac{d}{dt}{}^2{}_P\mathbf{r}^{P'}) = \begin{bmatrix} \breve H_1^x \\ \breve H_1^y \\ \breve H_1^z \end{bmatrix}_2, \quad \omega_b \times (\omega_b \times {}^P\mathbf{r}^{P'}) = \begin{bmatrix} \breve H_2^x \\ \breve H_2^y \\ \breve H_2^z \end{bmatrix}_2
$$

$$
\omega_a \times (\omega_a \times {}^{P'}\mathbf{r}^B) = \begin{bmatrix} \breve H_3^x \\ \breve H_3^y \\ \breve H_3^z \end{bmatrix}_2, \quad \omega_a \times (\omega_a \times {}^B\mathbf{r}^{G_b}) = \begin{bmatrix} \breve H_4^x \\ \breve H_4^y \\ \breve H_4^z \end{bmatrix}_2
$$

$$
\mathbf{H}_b = \mathbf{I}_b \omega_a = \begin{bmatrix} I_b^{xx}(-\dot\beta C_\gamma - \dot\psi S_\gamma S_\beta - \dot\theta) \\ I_b^{yy}(\dot\beta S_\gamma C_\theta - \dot\psi C_\gamma S_\beta C_\theta - \dot\psi S_\theta C_\beta) \\ I_b^{zz}(\dot\beta S_\gamma S_\theta - \dot\psi C_\gamma S_\beta S_\theta + \dot\psi C_\theta C_\beta) \end{bmatrix}_3
$$

VII. ACKNOWLEDGMENTS

The authors would like to thank the Equos Research Co., Ltd. for their help in providing valuable experimental data of a real vehicle.

REFERENCES

[1] R. Hibbard and D. Karnopp, "Twenty-First Century Transportation System Solutions: A New Type of Small, Relatively Tall and Narrow Active Tilting Commuter Vehicle", *Vehicle System Dynamics*, vol. 25, no. 5, pp. 321-347, 1996.

[2] J. Huang, Z. Guan, T. Matsuno, T. Fukuda and K. Sekiyama, "Sliding Mode Velocity Control of Mobile Wheeled Inverted Pendulum Systems", *IEEE Transactions. Robotics*, vol. 26, no. 4, pp. 750-758, 2010.

[3] F. Grasser, A. D'Arrigo, S. Colombi, and A. Rufer, "Joe: A mobile, inverted pendulum", *IEEE Trans. Ind. Electron*, vol. 49, no. 1, pp. 107-114, 2002.

[4] (2011). [Online]. Available: http://www.segway.com

[5] H. Tirmant, M. Baloh, L. Vermeiren, T. M. Guerra, and M. Parent, "B2, an alternative two wheeled vehicle for an automated urban transportation system", *Proc. IEEE Intell. Veh. Symp*, Paris, France, pp. 594-603, 2002.

[6] R.S. Sharp, "The Stability and Control of Motorcycles", *Journal of Mechanical Engineering Science*, vol. 13, no. 5, pp. 316-329, 1971.

[7] R.S. Sharp, "Stability, Control and Steering Responses of Motorcycles", *Vehicle System Dynamics*, vol. 35, no. 4-5, pp. 291-318, 2001.

[8] R.S. Sharp, "Advances in the Modelling of Motorcycle Dynamics", *Multibody System Dynamics*, vol. 12, no. 3, pp. 251-283, 2004.

[9] R. S. Sharp, "Research Note: The Influence of Frame Flexibility on the Lateral Stability of Motorcycles", *Mechanical Engineering Science*, vol. 16, no. 2, pp. 117-120, 1974.

[10] R. Rajamani, J. Gohl, L. Alexander and P. Starr, "Dynamics of Narrow Tilting Vehicles", *Mathematical and Computer Modelling of Dynamical Systems*, vol. 9, no. 2, pp. 209-231, 2003.

[11] S. Kidane, L. Alexander, R. Rajamani, P. Starr, and M. Donath, "Control System Design for Full Range Operation of a Narrow Commuter Vehicle", *ASME International Mechanical Engineering Congress and Exposition*, pp. 123-142, 2005.

[12] J. Gohl, R. Rajamani, P. Starr and L. Alexander, "Development of a Novel-Tilt Controlled Narrow Commuter Vehicle", (internal report), Department of Mechanical Engineering University of Minnesota, 2006.

[13] H. Baruh, "Analytical Dynamics", *McGraw-Hill*, p. 117, 1999.

[14] J. Yi, D. Song, A. Levandowski and S. Jayasuriya, "Trajectory Tracking and Balance Stabilization Control of Autonomous Motorcycles", *IEEE ICRA 2006*, pp. 2583-2589, 2006.

[15] J.J. Breuer, "Analysis of Driver-Vehicle-Interaction in An Evasive Manoueuvre - Results of Moose Test Studies", *16th Enhanced Safety of Vehicles (ESV) Conf*, Paper No: 98-S2-W-35, 1998.